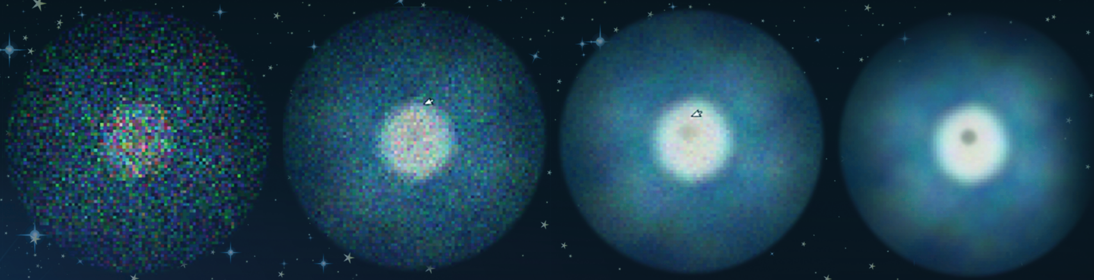

HIGH-RESOLUTION IMAGING

DETECTORS AND APPLICATIONS

Swapan K. Saha

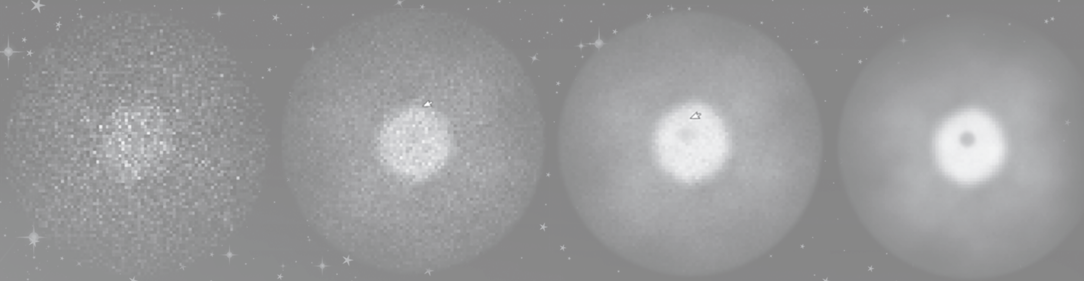

HIGH-RESOLUTION IMAGING

HIGH-RESOLUTION IMAGING

DETECTORS AND APPLICATIONS

Swapan K. Saha

Pan Stanford Publishing

Published by

Pan Stanford Publishing Pte. Ltd.
Penthouse Level, Suntec Tower 3
8 Temasek Boulevard
Singapore 038988

Email: editorial@panstanford.com
Web: www.panstanford.com

British Library Cataloguing-in-Publication Data
A catalogue record for this book is available from the British Library.

High-Resolution Imaging: Detectors and Applications

ISBN 978-981-4613-27-9 (Hardcover)
ISBN 978-981-4613-28-6 (eBook)

Printed in the USA

To my siblings
and
in memory of my parents

Contents

Preface

Existence of a quantum limit in light detection has led to a quest, on through the last century (and still going on), for the perfect detector that is asymptotically feasible. In 1901, Planck postulated that radiative transfers would occur by discrete packets of energy named “quanta,” following which in 1905, Einstein explained the photoelectric effect. The existence of photons means that for a given collecting area, there exists a physical limit on the minimum light intensity for any observed phenomenon. The perfect detector would be the one that is capable of detecting individual photo-event in the image plane.

The technology of developing detectors has evolved rather fast. The main application of such detectors is in the field of astronomy. Optical telescopes collect the radiation from the faint stellar objects, and the photons received from these objects are feeble. The situation becomes worse in the presence of atmospheric turbulence, particularly in the case of speckle imaging (Labeyrie, 1970) where post-detection data-processing algorithms are required to decipher diffraction-limited spatial Fourier spectrum and image features of such objects. In the early 1970s, the problem was the data processing; computers were not powerful enough for real-time processing and video recorders were expensive. Another application for such detectors is the signal sensing, especially wavefront sensing for adaptive optics (AO) and fringe tracking, which is important for long-baseline optical interferometry.

Research in solid-state electronic imaging detector commenced at the end of the 1960s. Boyle and Smith (1970) introduced the concept of charge-coupled device (CCD). Soon CCDs replaced TV camera tubes for the photon-counting cameras using image intensifiers. However, the possibility to have a fully solid-state photon-counting camera is quite recent. Modern detectors with (i) high sensitivity, (ii) high selectivity and detectivity, (iii) fast response, (iv) high efficiency, (v) low noise, and (vi) high read-out speed play a key role in astronomical applications. A photon-counting system allows the accurate photon centroiding and provides the dynamic range needed for measurements of source characteristics. At present, the large-format CCD and complementary metal oxide semiconductor array mosaics, electron-multiplication CCDs, electron avalanche photodiode arrays, quantum-well infrared photon detectors, etc., are available. However, the requirements of artifact-free photon shot-noise limited images include higher sensitivity and quantum efficiency, reduced noise that includes dark current, read-out and amplifier noise, smaller point spread functions, and higher spectral bandwidth.

The interest in using the image information in the form of coordinate sets came from the high-angular-resolution techniques (Saha, 1999, 2002, 2007, 2010; Labeyrie et al., 2006, and references therein) for astronomy, which require to take images with exposure times shorter than the atmospheric coherence time (see Section 1.5.3), which is, in general, less than 20 ms depending on the high altitude wind. At this exposure time, the signal-to-noise ratio in each frame is so low that image intensification is usually required. In view of the reasons stated above, I felt the necessity to write a monograph on the modern detector, though a chapter is dedicated on this topic in my first book entitled, *Diffraction-Limited Imaging with Large and Moderate Telescopes*, 2007, World-Scientific. At the fall of 2009, Dr. Stanford Chong, Director and Publisher, Pan Stanford Publishing Co., invited me, for which I am indebted to, for expanding the talk on this topic, which I delivered at AOMD-2008, India, into a book, which I duly complied with to accept the offer. Studded with tens of figures and footnotes, this book aims to address modern detecting systems, technologies and design, evaluation and calibration, control electronics, scientific applications, and results.

The first chapter deals with the fundamentals of important aspects, such as electromagnetic radiations, optical wavelengths in particular, emanating from the celestial sources and their distortions due to the optical elements and Earth's atmosphere while passing through to the detector. Also, discussed in brief are semiconductor physics and laser and its related phenomena in the second and third chapters, respectively. Chapters 4 through 6 address the photon detection process, photodetectors, and charge transfer devices. The photon-counting devices in the visible wavelength are discussed in the penultimate Chapter 7. The last but not the least, Chapter 8 presents the radiation detectors in infrared wavelengths. My recent interaction with a noted quantum physicist on multi-photon extension of intensity interferometry (Hanbury Brown, 1974) gives me hope that the book would kindle spirits to pursue the fields yet to benefit from the knowledge gained in these chapters. Barring the radio detection technique and intensity interferometry, which were elucidated at length in my second book entitled, *Aperture Synthesis: Methods and Applications to Optical Astronomy*, 2010, Springer, I have also highlighted the detector systems for high energies in brief in Chapters 5 and 7, since their use in astronomy as well as in medical sciences is noteworthy.

I am indebted to my PhD supervisor, late Prof. A. K. Sen, who initiated me into experimental science at the Institute of Radio Physics and Electronics, University of Calcutta. I express my gratitude to A. Labeyrie, S. K. Sarkar, A. Satya Narayanan, Kavita S. Rao, B. P. Pal, R. Ghosh, S. P. Bagare, S. S. Negi, R. Ramesh, M. S. Sundararajan, R. Srinivasan, and U. S. Kamath for assistance as readers of the draft chapters. Thanks are also due to G. P. Weigelt, R. Osterbart, I. S. McLead, A. Popowicz, S. Pal, Ya-Lin Wu, F. Malbet, P. Nisenson (late), V. Chinnappan, N. K. Rao, L. Close, S. Morel, A. Blazit, E. Pedretti, D. Mourard, D. Ives, K. B. Jinesh, N. Bezawada, A. R. Rao, J. Chatterjee, S. Ghosh, S. Srivastav, G. C. Anupama, D. Ojha, and S. Bhadra for providing the images, spectra, figures, etc., and granting permission for their reproduction. The services rendered by Baba A. Varghese, A. Surya, R. K. Sharma, S. P. Tewari, V. Valsan, R. Mondal, P. Anbazhagan, and S. K. Dhara are greatly acknowledged.

References

Boyle W. S. Smith G. E., 1970, *Bell System Tech. J.*, **49**, 587.

Hanbury Brown R., 1974, *The Intensity Interferometry: Its Applications to Astronomy*, Taylor & Francis, London.

Labeyrie A., 1970, *Astron. Astrophys.*, **6**, 85.

Labeyrie A., Lipson S. G., Nisenson P., 2006, *An Introduction to Optical Stellar Interferometry*, Cambridge University Press, UK.

Saha S. K., 1999, *Bull. Astron. Soc. Ind.*, **27**, 443.

Saha S. K., 2002, *Rev. Mod. Phys.*, **74**, 551.

Saha S. K., 2007, *Diffraction-limited Imaging with Large and Moderate Telescopes*, World-Scientific, New Jersey.

Saha S. K., 2010, *Aperture Synthesis: Methods and Applications to Optical Astronomy*, Springer, New York.

Swapan K. Saha
November 2014

Principal Symbols

A_{21}	Einstein coefficient for spontaneous emission
$\mathtt{A}_{\mathrm{d}}$	Effective area of the detector
$\mathbf{B}(\mathbf{r}, t)$	Time dependent magnetic field
B_{21}	Einstein coefficient for stimulated emission
$B_{\nu}(T)$	Spectral radiancy
$\mathcal{B}_{\mathrm{n}}(\mathbf{r})$	Covariance function
C	Capacitance
C	Coulomb
$\mathcal{C}_{\mathrm{n}}^2$	Refractive index structure constant
D	Diameter of the aperture
D^*	Specific detectivity
D_{e}	Diffusion coefficient of electrons
D_{h}	Diffusion coefficient of holes
$\mathbf{D}$	Electric displacement vector
$\mathcal{D}_{\mathrm{n}}(\mathbf{r})$	Refractive index structure function
E_{C}	Conduction band energy
E_{D}	Donor level energy
$\mathcal{E}_{\mathrm{e}}$	Irradiance
$\mathcal{E}_{\mathrm{e}}(\lambda)$	Spectral irradiance
E_{F}	Fermi level energy
E_{g}	Bandgap energy
E_{i}	Intrinsic Fermi level energy
E_{k}	Kinetic energy
$\mathcal{E}_{\nu}$	Illuminance
$erfc$	Error function
$\mathbf{E}(\mathbf{r}, t)$	Time dependent electric field
E_{V}	Valence band energy

F	Flux
f	Focal length
f_e	Effective focal length
f_G	Greenwood frequency
F_{max}	Maximum frame rate
$F_{\#}$	Aperture ratio
G	Gain
$\mathcal{G}$	Heat conductance
$\mathbf{H}$	Magnetic field
$\mathcal{H}$	Heat capacity
$\hat{H}$	Hamiltonian operator
$\hbar(= h/2\pi)$	Reduced Planck constant
I	Intensity of light
i	Current
i_B	Base current
i_C	Collector current
i_D	Dark current
i_d	Detector current
I_{DC}	Direct current
i_e	Electron current
i_E	Emitter current
$\mathcal{I}_e$	Radiant intensity
i_{FN}	Flicker noise current
i_h	Hole current
$\mathcal{I}_\lambda$	Spectral radiant intensity
$\mathcal{I}_\nu$	Luminous intensity
i_n	Dark current noise
i_{ph}	Photocurrent
i_Q	Shot-noise or quantum noise
i_s	Signal current
i_{sc}	Short-circuit signal current
$i(t)$	instantaneous photocurrent
i_0	Reverse saturated current
$\widehat{I}(\mathbf{u})$	Image spectrum
$\widehat{I}(\mathbf{x})$	Intensity distribution at the image plane
$\mathbf{J}$	Electric current density
$\mathbf{J}_d$	Drift current

$\mathbf{J}_{\text{diff}}$	Diffusion current
j	= 1, 2, 3
L_{e}	Diffusion length of electrons
L_{h}	Diffusion length of holes
L_0	Outer scale length
l	Characteristic size of viscous fluid
l_{c}	Coherence length
l_0	Inner scale length
$\mathcal{L}_{\text{e}}$	Radiance
$\mathcal{L}_{\nu}$	Luminance (brightness)
$\mathcal{L}_{\star}$	Stellar luminosity
M	Multiplication factor
$\mathtt{M}$	Magnification
$\mathcal{M}_{\text{e}}$	Radiant emittance
$\mathcal{M}_{\text{e}}$	Spectral radiant emittance
$\mathcal{M}_{\nu}$	Luminous emittance
$\mathcal{M}_{\text{q}}$	Photon emittance
$\mathcal{M}_{\text{q}}(\lambda)$	Spectral photon emittance
m_{v}	Apparent visual magnitude
M_{v}	Absolute visual magnitude
m^*	Effective mass
$M_{\star}$	Stellar mass
n	Refractive index
N	Integer value
N_{e}	Magnitude of free electron concentration
N_{h}	Magnitude of hole concentration
N_{pe}	Number of photoelectrons
N_{ph}	Number of photons
n_{ro}	Read-out noise
$n(\mathbf{r}, t)$	Refractive index of the atmosphere
$O(\mathbf{x})$	Object illumination
$\widehat{O}(\mathbf{u})$	Object spectrum
P	Pressure
$\mathcal{P}$	Probability distribution
$\mathbf{p}$	Momentum
P_{o}	Output optical power
P_0	Incident optical power

q	Electron charge
$\mathcal{Q}_{\mathrm{e}}$	Radiant energy
$\mathcal{Q}_{\lambda}$	Spectral radiant energy
$\mathcal{Q}_{\nu}$	Luminous energy
$\mathbf{r}(= x, y, z)$	Position vector of a point in space
R	Resistance
$\mathcal{R}$	Responsivity
$\mathcal{R}(\lambda)$	Spectral responsivity
$\mathcal{R}_{\nu}$	Luminous flux responsivity
R_{e}	Reynolds number
R_{f}	Entrance face reflectivity (Fresnel reflectivity)
R_{H}	Rydberg constant
r_0	Fried's parameter
$R_{\star}$	Stellar radius
$\hat{\mathbf{s}}$	Unit vector
$S(\mathbf{x})$	Point spread function
$\mathcal{S}_{\mathrm{r}}$	Strehl's ratio
$\langle\widehat{S}(\mathbf{u})\rangle$	Transfer function for long-exposure image
$\widehat{S}(\mathbf{u})$	Optical transfer function
$\lvert\widehat{S}(\mathbf{u})\rvert^2$	Modulus transfer function
sr	Steradian
$s(\lambda)$	Spectral response of the detector
t	Time
$t(x, y)$	Transmittance
T	Temperature
$\mathbf{u} = (u, v)$	Spatial frequency vector
V	Electrostatic potential
$\mathcal{V}$	Visibility
v_{a}	Average velocity of a viscous fluid
V_{br}	Breakdown voltage
v_{d}	Drift velocity
v_{g}	Group velocity
V_{oc}	Open-circuit voltage
v_{p}	Phase velocity
w	Width of depletion region
$\mathcal{W}$	Radiation power
$\mathbf{x}(= x, y)$	Two-dimensional (2-D) position vector
$Z_{\mathrm{j}}(\rho, \theta)$	Zernike polynomial of order j

Greek symbols

α	Extinction coefficient
α_{e}	Electron-ionization coefficient
α_{h}	Hole-ionization coefficient
β	Ratio of electron and hole mobilities
γ	Zenith angle
$\Gamma(\tau)$	FT of auto-correlation function
δ	Phase difference
$\delta(x)$	Dirac delta function
Δ	Relative core-cladding index difference
$\Delta\nu$	Spectral width
Δf	Electrical bandwidth
Δt	Integration time
ϵ_0	Permittivity in vacuum
ε	Energy dissipation
η_{d}	Quantum efficiency of the detector
Θ	Seebeck coefficient
θ	Angular diameter
θ_0	Isoplanatic angle
(θ, ϕ)	Polar coordinates
κ	Wave number
$\boldsymbol{\kappa}$	Wave vector
λ	Wavelength
λ_0	Wavelength in vacuum
μ_0	Permeability in vacuum
μ_{e}	Electron mobility
μ_{h}	Hole mobility
ν	Frequency
$\boldsymbol{\xi}(\xi, \eta)$	2-D position vector
$\langle\sigma\rangle$	Standard deviation
$\langle\sigma\rangle^2$	Variance
σ_{I}	Scintillation index
τ_0	Atmospheric coherence time
τ_{c}	Coherence time
τ_{d}	Response time
τ_{e}	Lifetime of electrons
τ_{g}	Group delay

τ_{h}	Lifetime of holes
τ_{r}	Total rise time
τ_{RC}	RC time-constant
τ_{w}	Delay time due to waveguide dispersion
ϕ_0	Work function
ϕ_{m}	Work function of metal
ϕ_{s}	Work function of semiconductor
Φ_{e}	Radiant power/flux
Φ_{λ}	Spectral radiant flux
Φ_{ν}	Luminous power/flux
$\Phi_{\mathrm{n}}(\boldsymbol{\kappa})$	Power spectral density
χ	Electron affinity
Ψ	Time-dependent wave-function
Psi_{B}	Potential difference between E_{F} and E_{i}
Ψ_{n}	Eigen functions
Ω	Solid angle
ω	Angular frequency
*	Complex operator
$\star$	Convolution operator
$\otimes$	Correlation
$\langle\ \rangle$	Ensemble average
$\widehat{}$	Fourier transform operator
$\boldsymbol{\nabla}$	Linear vector differential operator
∇^2	Laplacian operator

Some numerical values of physical and astronomical constants

c	Speed of light in free space	3×10^8 m.s^{-1}
c_1	First radiation constant	$2\pi hc^2 = 3.7418 \times 10^4$ Wμm^4.cm^{-2}
c_2	Second radiation constant	$hc/k_B = 1.4388 \times 10^4$ μm K
eV	Electron volt	1.60×10^{-19} J
h	Planck's constant	6.626096×10^{-34} J.s
Jy	Jansky	10^{-26} W m^{-2} Hz^{-1}
k_B	Boltzmann's constant	1.380662×10^{-23} J.K^{-1}
K_m	Luminous efficacy (photopic vision)	683 lm.W^{-1}
$\mathcal{L}_\odot$	Solar luminosity	3.839×10^{26} W
lx	Lux	lm.m^{-2}
$M_\odot$	Solar mass	1.9889×10^{30} kg
q	Elementary charge	1.6×10^{-19} C
R_L	Load resistance	
$R_\odot$	Solar radius	6.96×10^8 m
$T_\odot$	Solar effective temperature	5780 K
ϵ_0	Permittivity constant	8.8541×10^{-12} F.m^{-1}
μ_0	Permeability constant	1.26×10^{-6} H.m^{-1}
σ	Stefan–Boltzmann's constant	5.67×10^{-8} W m^{-2} K^{-4}

List of Acronyms

AC	Alternating current
ACT	Atmospheric Cerenkov Telescope
A/D	Analog-to-digital
AGN	Active galactic nuclei
AMBER	Astronomical Multiple BEam Recombiner
AO	Adaptive optics
APD	Avalanche photodiode
ASM	Adaptive secondary mirror
ASTROSAT	ASTROnomy SATellite
AT	Auxiliary Telescope
AU	Astronomical unit
BID	Blind iterative deconvolution
BJT	Bipolar junction transistor
BLIP	Background-limited performance
CCD	Charge coupled device
cd	Candela
CDS	Correlated double sampling
CHARA	Center for High Angular Resolution Astronomy
CIC	Clock-induced charge
CMOS	Complementary metal oxide semiconductor
CP40	Comptage de photon 40 mm
CPNG	Comptage de photon nouvelle gènèration
CPU	Central processing unit
COAST	Cambridge Optical Aperture Synthesis Telescope
CRT	Cathode ray tube
CS	Curvature sensor
CTE	Charge transfer efficiency
CTF	Contrast transfer function
CZT	Cadmium zinc telluride

CZTI	Cadmium zinc telluride imager
dB	Decibel
DC	Direct current
DM	Deformable mirror
DSP	Digital signal processor
EELT	European Extremely Large Telescope
EMCCD	Electron multiplying CCD
EMF	Electromotive force
ESA	European Space Agency
ESO	European Southern Observatory
FET	Field-effect transistor
FLUOR	Fiber-Linked Unit for Optical Recombination
FOV	Field-of-view
FPA	Focal plane array
FPGA	Field programmable gate array
FPS	Frames per second
FT	Fourier transform
FUSE	Far-Ultraviolet Spectroscopic Explorer
FWHM	Full width at half maximum
GALEX	Galaxy Evolution Explorer
G-APD	Geiger-mode APD
GI2T	Grand Interféromètre à deux Télescopes
GR	Generation-recombination
GRAVITY	General relativity analysis via VLT interferometry
HAGAR	High Altitude Gamma ray telescope ARray
HR	Hertzsprung-Russell
HAWAII	HgCdTe Astronomical Wide Area Infrared Imager
HCT	Himalayan Chandra Telescope
HST	Hubble Space Telescope
Hz	Hertz
IAO	Indian Astronomical Observatory
IC	Integrated circuit
ICCD	Intensified CCD
IF	Intermediate frequency
IO	Integrated optics
IONIC	Integrated optics near-IR combiner
IOTA	Infrared Optical Telescope Array

IPCS	Image Photon-Counting System
IR	Infrared
IRAF	Image Reduction and Analysis Facility
IRAS	InfraRed Astronomical Satellite
IRTS	InfraRed Telescope in Space
ISI	Infrared Spatial Interferometer
ISM	Interstellar medium
ISO	Infrared Space Observatory
I2T	Interféromètre à deux Télescopes
ITF	Intensity transfer function
kV	Kilovolt
Laser	Light amplification by stimulated emission of radiation
LBOI	Long-baseline optical interferometry
LBT	Large Binocular Telescope
LBV	Luminous blue variable
LCD	Liquid crystal display
LED	Light-emitting diode
LGS	Laser guide star
LHS	Left hand side
LIGO	Laser Interferometer Gravitational-Wave Observatory
LSF	Line spread function
LO	Local oscillator
L3CCD	Low light level CCD
LWIR	Long-wave infrared
ly	Light year
mA	Milli-ampere
MAMA	Multi Anode Micro-channel Array
mas	Milliarcseconds
Maser	Microwave amplification by stimulated emission of radiation
MBE	Molecular beam epitexy
MCP	Micro-channel plate
MCT	Mercury cadmium telluride
MHz	Megahertz
MIRC	Michigan Infra-Red Combiner
MMDM	Micro-machined DM
MMF	Magnetomotive force
MO	Microscope objective

MOS	Metal-oxide semiconductor
MOSFET	Metal-oxide semiconductor FET
MOSFIRE	Multi-Object Spectrometer for InfraRed Exploration
MMT	Multi Mirror Telescope
MRI	Magnetic resonance imaging
MSGIS	Mammary Gland Specific Gamma Imaging System
MTF	Modulation transfer function
MWIR	Mid-wave infrared
NA	Numerical aperture
NASA	National Aeronautics and Space Administration
NEA	Negative electron affinity
NEAT	Nearby Earth Astrometric Telescope
NEΔT	Minimum detectable temperature difference
NEP	Noise equivalent power
NETD	Noise equivalent temperature difference
NICMOS	Near Infrared Camera and Multi-Object Spectrometer
NIRSPEC	Near Infrared echelle Spectrometer
nm	Nanometer
OCT	Optical coherence tomography
Op-Amp	Operational amplifier
OPD	Optical path difference
OTF	Optical transfer function
PAPA	Precision Analog Photon Address
PAVO	Precision Astronomical Visible Observations
pc	Parsec
PC	Photoconductive
PDS	Photometric data system
PE	Photoemissive
PEM	Photoelectromagnetic
PHD	Pulse height distribution
pixel	PICture ELement
PMT	Photomultiplier tube
POSS	Palomar Observatory Sky Survey
PSD	Position-sensing device
PSF	Point spread function
PSPMT	Position sensitive photomultiplier technology
PTF	Phase transfer function
PV	Photovoltaic

PZT	Piezo-electric transducer
QE	Quantum efficiency
QDIP	Quantum dot IR photodetector
QWIP	Quantum well IR photodetector
RHS	Right hand side
RMS	Root-mean-square
ROIC	Read-out integrated circuit
SAO	Special Astrophysical Observatory
SH	Shack–Hartmann
SL	Super-lattice
SLS	Strained layer super-lattice
S/N	Signal-to-noise
sr	Steradian
STJ	Superconducting tunnel junction
SUSI	Sydney University Stellar Interferometer
SWIR	Short-wave infrared
SXT	Soft X-ray Telescope
TC	Triple-correlation
TDI	Time-delay and integration
TMT	Thirty Meter Telescope
TSM	Tomographic speckle imaging
TV	Television
UT	Unit Telescope
UV	Ultra-violet
UVIT	Ultra-Violet Imaging Telescope
VBO	Vainu Bappu Observatory
VBT	Vainu Bappu Telescope
VEGA	Visible spEctroGraph and polArimeter
VINCI	VLT INterferometer Commissioning Instrument
VLTI	Very Large Telescope Interferometer
WFS	Wavefront sensor